Parallel Raman microspectroscopy using programmable multipoint illumination

Ji Qi* and Wei-Chuan Shih

Department of Electrical & Computer Engineering, University of Houston 4800 Calhoun Rd., Rm N308 Eng. Bldg 1, Houston, Texas 77204, USA

**Corresponding author: wshih@uh.edu*

Received February 22, 2012; revised February 28, 2012; accepted February 28, 2012; posted February 29, 2012 (Doc. ID 163450); published April 4, 2012

We present a novel parallel Raman microspectroscopy scheme for simultaneously collecting Raman spectra from multiple points. This scheme is realized by projectinga multiple-point laser illumination pattern using a spatial light modulator (SLM) and wide-field Raman imaging collection. We demonstrate the performance of this scheme using uniform samples, trapped polymer microparticles and fixed polymer microparticles with mixed molecular composition within a 50×50 μm^2 field of view. This scheme enables the acquisition of Raman spectra from as many as 40 points simultaneously using a single illumination pattern and detector recording frame without scanning.

OCIS codes: 300.6230, 110.4234, 350.4855.

Raman spectroscopy can provide molecular information via inelastic light scattering without physical contact. Coupled with microscopic imaging, Raman microspectroscopy is a powerful technique for material analysis, for example, stress and temperature measurement in silicon and compositional analysis of polymer microparticles [1]. Three methodologies are commonly employed in contemporary Raman microspectroscopy, namely, point-scan, line-scan and global illumination [1].

The point-scan operation involves the collection of Raman spectra in a point-by-point fashion. Since Raman scattering is a relatively weak phenomenon, the laser spot dwelling time at each point is typically on the order of milliseconds to seconds. In addition, the data needs to be read-out after each point acquisition, which typically adds another few hundred milliseconds for a standard charge-coupled device (CCD) detector. As a result, conventional point-scan Raman mapping is a time-consuming process and can take as long as a few hours to map a 50×50 μm^2 region.

To improve efficiency, parallel acquisition has been implemented based on time-sharing or power-sharing schemes. In the former, the laser is rapidly scanned over multiple points of interest during the time of a single CCD recording frame [2,3]. In the latter, the laser is shaped into an elongated line and the entire line is imaged by a single CCD frame [1,4,5]. Thus, both schemes can substantially reduce multiple read-out times. A key difference, however, lies in the temporal power fluctuation within a CCD frame: For time-sharing, the total laser power is focused on one spot at any given time but for power-sharing the laser power is distributed on all spots. Therefore, the frame-averaged power is identical to the instantaneous power for power-sharing but not for time-sharing. Another significant difference is there is no scanning within each frame for power-sharing. Recently, the time-sharing approach has been demonstrated to provide flexibility for imaging multiple points not aligned on a line, which is particularly advantageous for sparse samples such as bacteria or environmental particles [2].

In this letter, we present a novel power-sharing approach that allows the simultaneous imaging of multiple points not aligned on a line. This is achieved by combining programmable multi-point laser illumination with wide-field Raman imaging. Our scheme can significantly improve the sampling flexibility compared to the line-shaped illumination approach while maintaining the parallel acquisition efficiency, 100% laser power duty cycle on all spots, and the non-scanning nature within a single CCD frame. Although imaging multiple spots simultaneously using a spatial light modulator (SLM) has been developed for multi-photon fluorescence microscopy [6], it has not been implemented in Raman microspectroscopy.

The system configuration is shown in Fig. 1(a). The 785 nm output of a CW Titanium:Sapphire laser (Spectra-Physics 3900 S) is filtered by a laser-line filter (Semrock LL01-785-12.5) and expanded to ~1 cm in diameter before the spatial light modulator {(SLM) liquid crystal on silicon (LCOS) Hamamatsu}. The output from the SLM is fed through the back port of an inverted microscope (Olympus IX71) with an addition of a tube lens. A dichroic mirror (Semrock LPD01-785RU-25) is placed in the microscope turret for epi-Raman acquisition via a microscope objective (Olympus UPLSAPO 60XW, 1.2 NA). The Raman light is redirected out via the microscope side port, filtered by a long-wave pass filter (Semrock LP02-785RS-25), and sent into a spectrograph (Acton SpectroPro 300i) with a thermal-electrically cooled CCD camera (Princeton 400BR-excelon). We use the code developed by Grier's group to program the SLM to generate illumination patterns [7]. The CCD data acquisition and the SLM pattern generation are synchronized by Labview (National Instruments). The spectral resolution of our system is ~8 cm^{-1} by comparing spectra taken by this system and a calibrated confocal Raman system, respectively. As shown in Fig. 1(b), the Raman spectra of polystyrene (PS) and polymethylmethacrylate (PMMA) are measured by both systems and no appreciable differences are noticed. The spatial (x-y-z) resolution is ~0.9, 0.9 and 4.5 μm, respectively at 785 nm excitation using 0.5 μm PS beads fixed on a glass coverslip [Figs. 1(c)–1(e)]. We first demonstrate the performance of our scheme using a uniform silicon sample. The patterns shown in Figs. 2(a)–2(c) are the raw images

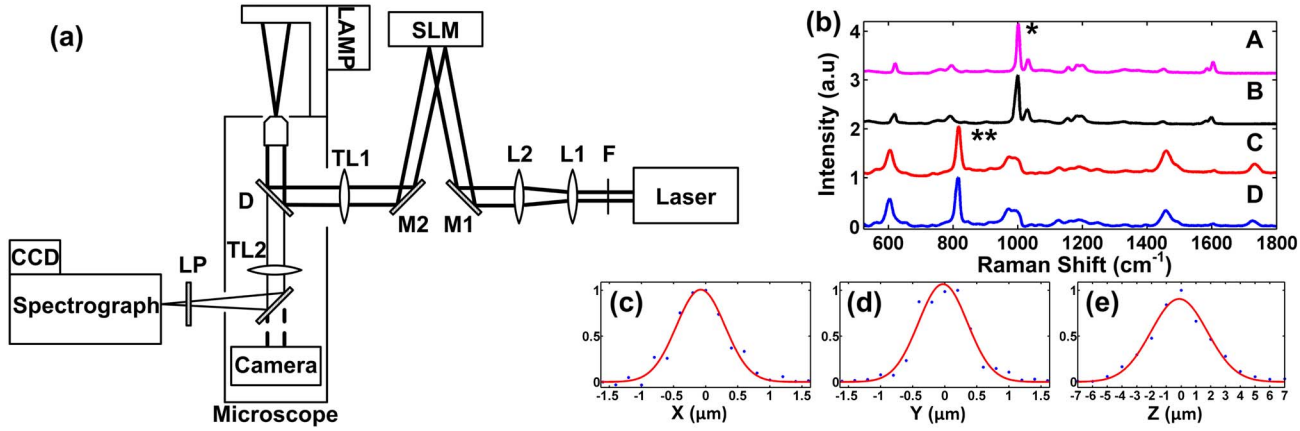

Fig. 1. (Color online) (a) System configuration: laser line filter (F); beam expander (L1/L2); spatial light modulator (SLM); mirrors (M1/M2); tube lenses (TL1/TL2); dichroic beamsplitter (D); long-wave pass filter (LP); (b) Raman spectra of PS (A) and PMMA (C) measured using the proposed system vs. PS (B) and PMMA (D) measured by a confocal Raman system with spectral resolution ~8 cm^{-1}; spatial resolution in (c) x, (d) y and (e) z direction.

cropped from the 520 cm^{-1} silicon Raman peak region after polynomial-based background removal. Since there are no other Raman features near this peak, these Raman images appear to be identical to the illumination pattern with slight additional spread in the x direction due to dispersion. A design constraint on the illumination pattern is that no two points are allowed to completely overlap along the direction perpendicular to the grating dispersion direction, preventing data mixing from adjacent points.

Next, we analyze a mixed population of a total of 138 PS and PMMA microparticles (each 3 μm in diameter, Sigma—Aldrich). A snapshot visual image in Fig. 3(a) shows little difference between them even though the index of these two materials are quite different (PS 1.55–1.59; PMMA ~1.49). Using a centroid finding algorithm over the snapshot image, we first identify the center of individual microparticles. Then the centroids are grouped into 11 sub-groups, resulting in 11 patterns as the SLM input. For example, pattern no. 5 is shown in Fig. 3(b) with the laser spots overlaid with 17 microparticles. After collecting the Raman spectra from all microparticles, chemical identification can be made by using the characteristic Raman features of PS and PMMA, e.g., the peaks marked out in Fig. 1(b) with results shown in Fig. 3(c) where PS beads are marked red. We note that due to the relatively large size of the particles compared to the laser spot size, more patterns are needed to satisfy the no overlapping constraint mentioned earlier. With smaller particles, our current field of view (~60×60 μm^2) would allow ~30 points per pattern without overlapping.

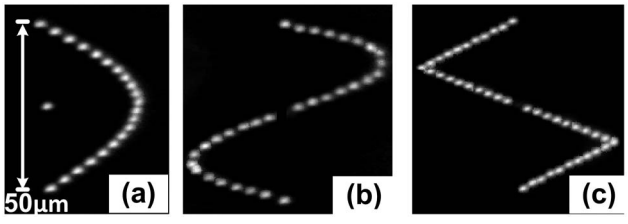

Fig. 2. 20-, 30- and 40-point illumination patterns: (a) half-sine; (b) full-sine; and (c) triangular patterns using the Raman peak of Si @ 520 cm^{-1}.

The previous example demonstrates a scenario when the microparticles are densely packed. We then prepare a different sample with sparse particle distribution (28 PS particles) as shown in Fig. 4(a). Following a similar scheme, complete chemical identification can be achieved using three patterns. Figure 4(b) shows the grouping scheme for the three illumination patterns. Figure 4(c) shows the corresponding Raman image using the PS Raman peak at 1001 cm^{-1} by overlaying all three frames. We note that the first illumination pattern has 17 points and each one is significantly dimmer than those in the second (6 points) and the third (5 points) patterns. This is due to the laser power distribution among more points. Next we assess the intensity uniformity within each pattern by measuring the silicon Raman peak (@520 cm^{-1}) intensity using a uniform silicon sample.

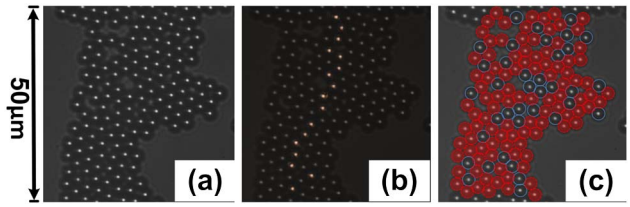

Fig. 3. (Color online) (a) Visual image of mixed population of PS and PMMA; (b) laser spots from pattern no. 5 overlaid with the visual image; (c) identification of PS and PMMA microparticles.

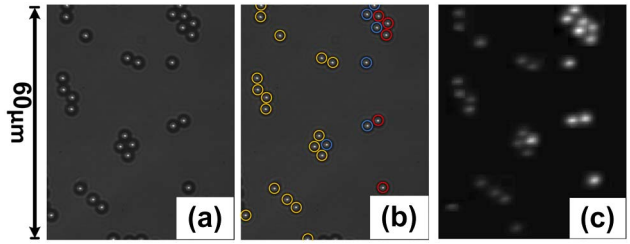

Fig. 4. (Color online) (a) Visual image of 28 PS microparticles; (b) grouping scheme for the 3 projected patterns (17-6-5) overlaid with the visual image; (c) resulting overlaid Raman image from three illumination patterns.

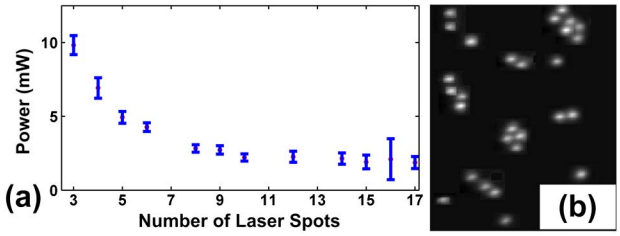

Fig. 5. (Color online) (a) Average intensity and standard deviation versus the number of laser spots in the 11 SLM patterns employed in Fig. 3; (b) intensity corrected Raman image corresponding to the raw image in Fig. 4(c).

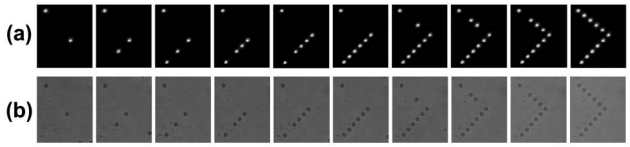

Fig. 6. Simultaneous trapping and Raman imaging of 2 to 11 PS microparticles: (a) PS Raman image and (b) visual image (Media 1).

Together with measuring the laser power, we can assess the image intensity uniformity across patterns with different number of points. Figure 5(a) shows the average power and standard deviation per point versus the number of points in the 11 SLM patterns employed in Fig. 3 with the same total laser power (100 mW before the SLM; ~30 mW at the sample). A gradual decrease in power per point is observed when more points are included in the illumination pattern.

The silicon data in Fig. 5(a) can be employed for intensity calibration within an illumination pattern as well as across different patterns with variable number of points. For example, Fig. 5(b) shows an intensity-corrected PS image corresponding to the raw image shown in Fig. 4(c), indicating remarkable improvement.

Since tightly focused laser spots can readily form optical traps, the proposed scheme can trap multiple polystyrene beads in a non-straight line as shown in Fig. 6(a)–6(b) [7]. To generate the Raman image, we have employed the PS Raman spectrum and the major peak intensity of 1001 cm^{-1} as marked with an asterisk in Fig. 1(b) (Media 1). We note that a potential advantage of the proposed scheme is its trapping stability against flow due to the 100% illumination duty cycle during trapping, i.e., constant optical gradient is maintained without instantaneous power fluctuations. An on-line movie shows effective trapping against background flow as evidenced by the motion of untrapped microparticles (Media 2). The proposed scheme can also trap multiple microparticles at different depths as shown in Fig. 7(a) with the raw images of PMMA's Raman peak at 813 cm^{-1} from two beads with 5 μm separation shown in Fig. 7(b). Apparently the spectrum from the out-of-focus bead is blurred,

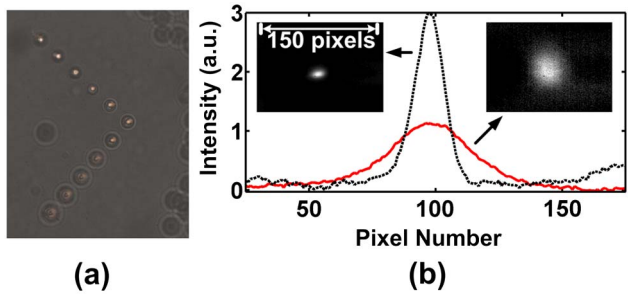

Fig. 7. (Color online) Multiple traps at different depths: (a) laser spots overlaid on 11 PMMA microparticles at different zs; (b) Raman intensity on the CCD of the in-focus (dotted) and out-of-focus (solid) PMMA microparticles by binning all rows (Media 2).

however, this could be improved via deconvolution techniques.

In conclusion, we have demonstrated a novel scheme for parallel Raman microspectroscopy by combining programmable multi-point illumination and wide-field Raman imaging. This scheme provides flexibility to simultaneously image multiple points not aligned along a line in contrast to traditional power-sharing scheme using a line-shape illumination while retaining other features such as non-scanning, 100% duty cycle and constant power distribution on all spots within one CCD frame. This novel scheme may be applicable for ultra-high throughput Raman microspectroscopy and imaging, particularly when the sample is sparse or has unevenly distributed information density. In addition, this scheme can be effectively combined with optical traps with 100% duty cycle for facile multiplexed trapping and simultaneous Raman microspectroscopy.

Wei-Chuan Shih acknowledges funding support from the National Science Foundation (NSF) CAREER Award (CBET-1151154) and Cullen College of Engineering at the University of Houston.

References

1. S. Schlucker, M. D. Schaeberle, S. W. Huffman, and I. W. Levin, Anal. Chem. **75**, 4312 (2003).
2. L. Kong, Z. P, P. Setlow, and Y. Li, J. Biomed. Opt. **16**, 120503 (2011).
3. R. Liu, D. S. Taylor, D. L. Matthews, and J. W. Chan, Appl. Spectrosc. **64**, 1308 (2010).
4. J. Qi, P. Motwani, J. Wolfe, and W.-C. Shih, Proc. SPIE **8219**, 821903 (2012).
5. K. A. Christensen and M. D. Morris, Appl. Spectrosc. **52**, 1145 (1998).
6. V. Nikolenko, B. O. Watson, R. Araya, A. Woodruff, D. S. Peterka, and R. Yuste, Front. Neural Circuits **2**, 14 (2008).
7. J. E. Curtis, B. A. Koss, and D. G. Grier, Opt. Commun. **207**, 169 (2002).